

# SP1-induced lncRNA TUG1 regulates proliferation and apoptosis in islet cells of type 2 diabetes mellitus *via* the miR-188-3p/FGF5 axis

P. ZHANG<sup>1,2</sup>, Y.-N. LI<sup>3</sup>, S. TU<sup>2</sup>, X.-B. CHENG<sup>1</sup>

<sup>1</sup>Department of Endocrinology, the First Affiliated Hospital of Soochow University, Suzhou, China

<sup>2</sup>Department of Emergency, Wuxi Second Hospital Affiliated to Nanjing Medical University, Wuxi, China

<sup>3</sup>Department of Gastroenterology, Affiliated Hospital of Jiangnan University, Wuxi, China

*Ping Zhang and Yining Li contributed equally to this work*

**Abstract. – OBJECTIVE:** To elucidate the role of TUG1 in the onset of type 2 diabetes mellitus (T2DM) and the potential mechanism.

**MATERIALS AND METHODS:** Relative levels of TUG1 and SP1 in high-fat diet animal model and high-glucose cell model were detected by quantitative Real Time-Polymerase Chain Reaction (qRT-PCR), and their correlation was analyzed. Potential binding sites in the promoter sequences of TUG1 and SP1 were predicted using the JASPAR. Their interaction was further confirmed by chromatin immunoprecipitation (ChIP) and Dual-Luciferase reporter assay. The influences of TUG1 on proliferative and apoptotic potentials in Min6 cells were examined by Cell Counting Kit-8 (CCK-8), 5-Ethynyl-2'-deoxyuridine (EdU) assay and flow cytometry, respectively. Subsequently, the interaction in the TUG1/miR-188-3p /FGF5 axis was similarly explored by Dual-Luciferase reporter assay.

**RESULTS:** SP1 and TUG1 were downregulated in high-fat and high-glucose models, and they displayed a positive correlation. TUG1 bound E2 region in SP1 promoters. Knockdown of TUG1 inhibited proliferative rate and induced apoptosis in high-glucose-treated Min6 cells. Furthermore, the TUG1 / miR-188-3p /FGF5 axis was identified to be responsible for regulating Min6 cell functions.

**CONCLUSIONS:** SP1 induces TUG1 downregulation in T2DM cell models, which further regulates proliferative and apoptotic potentials in islet cells by activating the miR-188-3p/FGF5 axis.

*Key Words:*

T2DM, SP1, TUG1, MiR-188-3p, FGF5.

## Introduction

Type 2 diabetes mellitus (T2DM) is a chronic metabolic disorder featured by hyperglycemia. The pathogenesis of T2DM can be attributed to insulin resistance and/or islet dysfunction. Genetic, environmental and racial factors are all risk factors for increasing the susceptibility to T2DM. Insulin resistance induces compensatory increase of insulin secretion by islet  $\beta$  cells. However, the long-term compensation will eventually lead to deficiency of insulin secretion, thus causing abnormal glucose tolerance and T2DM<sup>1</sup>. Transcription regulation is of great significance in pancreas development<sup>2</sup>, islet differentiation<sup>3</sup> and insulin synthesis<sup>4</sup>. It is reported that transcription factors associated with islet  $\beta$  cell functions are involved in T2DM<sup>5</sup>. A large number of studies have later proposed that noncoding RNAs are involved in the regulation of islet functions<sup>6,7</sup>.

More than 98% of sequences in human genomes can be transcribed. Among them, most of genes with transcriptional activities cannot encode proteins, and they are finally transcribed to non-coding RNAs<sup>8</sup>. In the past, noncoding RNAs are considered as dark matters. However, they are not non-functional since noncoding RNAs have not been eliminated during the biological evolution. Current studies have indicated that noncoding RNAs are closely linked to human diseases, and their biological functions need further concerned<sup>9</sup>.

Long non-coding RNAs (lncRNAs) exert developmental specificity during the maturation of islet  $\beta$  cells. Moran et al<sup>10</sup> discovered 1,128

specifically expressed lncRNAs in human islet  $\beta$  cells. Among them, six lncRNAs are abundantly expressed only in mature cells, rather than human embryonic pancreatic progenitor cells, indicating that lncRNAs participate in regulating the differentiation and maturation of endocrine cells. Bramswig et al<sup>11</sup> suggested that islet-specific lncRNAs differ from cell types. Some lncRNAs are specifically expressed in  $\beta$  cells, while others are expressed in  $\alpha$  cells.

lncRNA TUG1 is abnormally expressed in colorectal cancer, prostate cancer and osteosarcoma<sup>12-14</sup>. Its involvement in T2DM progression is unclear, which is explored in this paper.

## Materials and Methods

### Experimental Mice

Animal experiments were strictly performed in accordance with the management proposed by the Soochow University Experimental Animal Committee and the Animal Ethics Committee approval. Mice were randomly assigned into NFD (n=15) and HFD (n=15) group. After one-week habituation, normal-fat diet (NFD: 10% fat, 70% carbohydrate, 20% protein, 3.85 kcal/gm, D12450B) and high-fat diet (HFD: 60% fat, 20% carbohydrate, 20% protein, 5.24 kcal/gm, D12492i) were given to mice until the 18<sup>th</sup> week. Five mice were placed in one cage and they were housed in a standard environment with 21±2°C and 12 h light/dark cycle.

### Cell Culture

The mouse islet  $\beta$  cell line Min6 exerts insulin secretion function that is similar to islet  $\beta$  cells, and it is widely used in experimental studies for analyzing islet  $\beta$  cell functions. Min6 cells were cultured in Dulbecco's Modified Eagle's Medium (DMEM; Gibco, Rockville, MD, USA) containing 15% fetal bovine serum (FBS) (Gibco, Rockville, MD, USA), 2.5 mM  $\beta$ -mercaptoethanol, 100 U/mL penicillin, 100  $\mu$ g / mL streptomycin, 10 mM HEPES, 1 mM sodium pyruvate, and 11.1 mM glucose. Fresh medium was replaced every 1-2 days, and cell passage was conducted when cell confluence reached 80-90%.

### Quantitative Real-Time Polymerase Chain Reaction (qRT-PCR)

Tissues were stored in liquid nitrogen, washed in phosphate-buffered saline (PBS) once and lysed in RNA lysate. Tissue mixture was incubated

in chloroform and centrifuged for 15 min. The supernatant was mixed in 200  $\mu$ L of absolute ethanol, and subjected to column centrifugation twice. Incubation with RNA Wash Buffer I and centrifugation for 30 s were conducted twice, followed by incubation with RNA Wash Buffer II. Finally, RNAs were eluted by centrifugation and subjected to qRT-PCR. Primer sequences were listed as follows: miR-188-3p: forward, 5'-TCTTGGTCCGCATGTGTGTG-3'; reverse, 5'-AGGGAGTTCAAAGGCAGCATG-3'; GAPDH, forward, 5'-ACATCATCCCTGCATCACT-3'; reverse, 5'-GTCCTCAGTGTAGCCCAAG-3'; TUG1: forward, 5'-TAGCAGTTC-CCCAATCCTTG-3'; reverse, 5'-CACAAATTC-CCATCATTCCC-3'; SP1: forward, 5'-GCCGTTG-GCTATAGCAAATGC-3'; reverse, 5'-CATATAC-GGGCATGAACACACATT-3'; FGF5: forward, 5'-CCCGGATGGCAAAGTCAATGG-3'; reverse, 5'-TTCAGGGCAACATACCCTCCCG-3'.

### Dual-Luciferase Reporter Assay

Luciferase vectors WT, MT1, MT2, MT3, MT4, MT5 were generated based on the predicted binding sites using the JASPAR, which were co-transfected into cells with plasmids using Lipofectamine RNA iMAX (Invitrogen, Carlsbad, CA, USA). Forty-eight hours later, Luciferase activity was measured.

### Chromatin Immunoprecipitation (ChIP)

ChIP assay was conducted using EZ-Magna ChIP<sup>TM</sup> G (Millipore, Billerica, MA, USA). Cells inoculated in 10-cm culture dishes were incubated with 280  $\mu$ L of 37% formaldehyde for 10 min, sonicated (10 s  $\times$  5) and centrifuged at 4°C, 12,000 r/min for 10 min. After removal of insoluble precipitation, 2  $\mu$ L of antibodies and 20  $\mu$ L of magnetic bead suspension were rotated with the mixture at 4°C overnight. Immunoprecipitation enrichment was determined by qRT-PCR with the input as a negative control.

### Cell Counting Kit-8 (CCK-8) Assay

Cells were inoculated in a 96-well plate with  $2 \times 10^3$  cells per well. At the appointed time points, absorbance value at 450 nm of each sample was recorded using the CCK-8 kit (RIBOBIO, Guangzhou, China) for plotting the viability curves.

### Cell Induction and Transfection

After 4-h induction in 5 mM glucose, Min6 cells were incubated with normal glucose (NG, 5 mM glucose) or high-glucose (HG, 25 mM

glucose) for 24 h. Twenty-four hours prior to transfection, Min6 cells were cultivated in antibiotics-free medium to 60-70% confluence, and transfected with diluted plasmids in Opti-MEM using Lipofectamine RNA iMAX. Transfection plasmids (pcDNA-SP1, TUG1 shRNA 1-3, miR-188-3p mimics, miR-188-3p inhibitor and negatively controls) were provided by GenePharma (Shanghai, China).

#### **5-Ethynyl-2'-Deoxyuridine (EdU) Assay**

Cells were pre-inoculated in a 24-well plate ( $2 \times 10^4$  cells/well). They were incubated in 4% methanol for 30 min, followed by 10-min permeabilization in 0.5% TritonX-100, and 30-min reaction in 400  $\mu$ L of 1 $\times$ ApollorR (RIBOBIO, Guangzhou, China). Afterwards, cells were dyed in 1 $\times$ Hoechst 33342 for another 30 min. Positive EdU-stained cells were calculated.

#### **Flow Cytometry**

Cell suspension at the density of  $1 \times 10^6$  cells/mL was prepared. Cells were re-suspended in 0.5 mL of pre-cooled 1 $\times$ binding buffer and 1.25  $\mu$ L of Annexin V-FITC (fluorescein isothiocyanate) (BD Biosciences, Detroit, MI, USA) in the dark for 15 min incubation. After centrifugation at 1000 $\times$ g for 5 min, the precipitant was re-suspended in 0.5 mL of pre-cooled 1 $\times$ binding buffer and 10  $\mu$ L of Propidium Iodide (PI) in the dark, followed by flow cytometry detection (FACSCalibur; BD Biosciences, Detroit, MI, USA).

#### **Statistical Analysis**

Statistical Product and Service Solutions (SPSS) 18.0 (SPSS Inc., Chicago, IL, USA) was used for statistical analysis. Spearman's rank correlation coefficient was carried out for assessing the relationship between expression levels of two genes. Differences between two groups were analyzed by using the Student's *t*-test. Comparison between multiple groups was done using One-way ANOVA test followed by Post-Hoc Test (Least Significant Difference). Data were expressed as mean  $\pm$  standard deviation, and  $p < 0.05$  was considered as statistically significant.

## **Results**

#### **SP1 and TUG1 Were Downregulated in HG-Treated Min6 Cells**

Compared with mice in NFD group, TUG1 level was markedly downregulated in mice of

HFD group (Figure 1A). In addition, TUG1 was downregulated in HG-treated Min6 cells as well (Figure 1B). According the prediction using the JASPAR, transcription factor SP1 may bind in the promoter region of TUG1 (Figure 1B). We subsequently mutated 5 possible binding sequences in the TUG1 promoter region (Figure 1C). SP1 was downregulated in mice of HFD group (Figure 1D) and Min6 cells of HG group (Figure 1E). SP1 level was positively correlated to that of TUG1 (Figure 1F). The 5 generated mutant-type TUG1 vectors were co-transfected in cells with pcDNA-SP1 or negative control. Dual-Luciferase reporter assay uncovered that the mutant-type 2 TUG1 vector could not activate the transcription of TUG1, suggesting that the actual binding between TUG1 and SP1 was in the E2 region (Figure 1G). ChIP assay further identified the binding between SP1 and TUG1 in the E2 region (Figure 1H). Consistently, transfection of pcDNA-SP1 markedly upregulated TUG1, proving their positive interaction (Figure 1I).

#### **Knockdown of TUG1 Inhibited Proliferative Ability in HG-Induced Min6 Cells and Induced Apoptosis**

To clarify the role of TUG1 in T2DM, we generated three lines of TUG1 shRNA. Among them, transfection efficacy of shRNA-2 was the best and it was used in the following experiments (Figure 2A). HG induction markedly decreased viability and EdU-positive rate in Min6 cells, which were further inhibited by knockdown of TUG1 (Figure 2B, 2C). Flow cytometry results revealed an increased apoptosis rate in HG-induced Min6 cells. Moreover, knockdown of TUG1 markedly increased apoptosis rate in HG-induced Min6 cells (Figure 2D). The above data suggested that TUG1 could regulate islet  $\beta$  cell functions.

#### **TUG1 Negatively Regulated MiR-188-3p Level**

Using the bioinformatics tool, we predicted potential miRNAs binding TUG1. The binding sites in the seed sequence of TUG1 and miR-188-3p were predicted (Figure 3A). Luciferase vectors were constructed based on the binding sites, and they were co-transfected into cells with miR-188-3p mimics or negative control, respectively. It is shown that overexpression of miR-188-3p markedly inhibited Luciferase activity in the wild-type TUG1 vector, and the Luciferase activity was not influenced in the mutant-type one (Figure

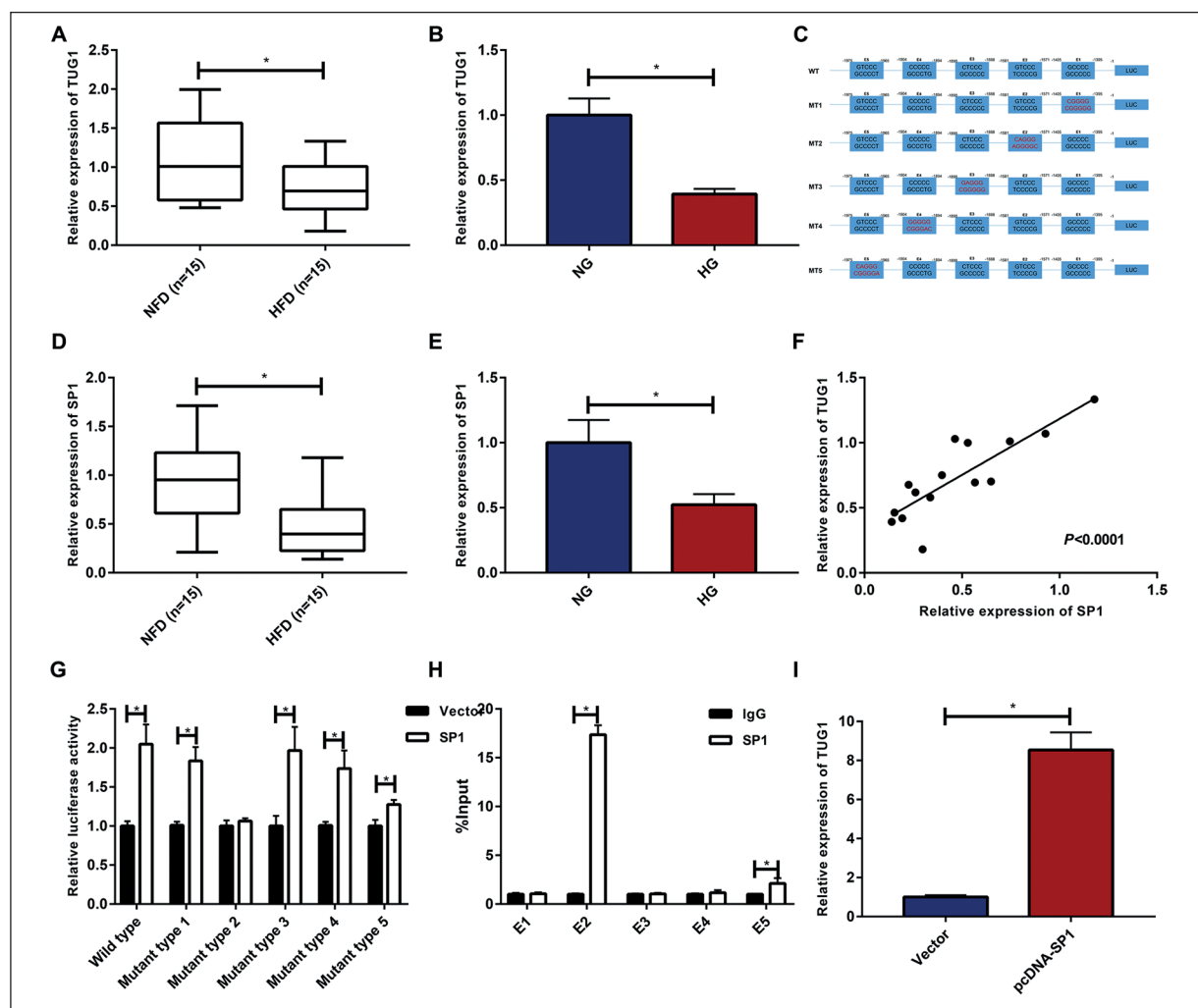


**Figure 1.** SP1 and TUG1 were downregulated in HG-treated Min6 cells. **A**, LncRNA TUG1 levels in mouse islet of NFD and HFD group detected by qRT-PCR. **B**, LncRNA TUG1 levels in NG or HG-induced Min6 cells detected by qRT-PCR. **C**, Five binding sites in the seed sequence of SP1 and TUG1. **D**, SP1 levels in mouse islet of NFD and HFD group detected by qRT-PCR. **E**, SP1 levels in NG or HG-induced Min6 cells detected by qRT-PCR. **F**, A positive correlation between TUG1 and SP1 levels in mouse islet of HFD group analyzed by Spearman's rank correlation coefficient. **G**, Luciferase activity in 5 mutant-type vectors of SP1; **H**, Enrichment of TUG1 in E1-E5 anti-SP1. **I**, TUG1 level in Min6 cells transfected with pcDNA-SP1; \* $p < 0.05$ .

3B). Knockdown of TUG1 in Min6 cells upregulated miR-188-3p, and overexpression of TUG1 resulted in the opposite trend (Figure 3C, 3D). As expected, TUG1 and miR-188-3p displayed a negative correlation (Figure 3E).

#### MiR-188-3p Negatively Regulated FGF5

Using the same method, FGF5 was identified to be the target gene binding miR-188-3p (Figure 4A, 4B). FGF5 level was negatively regulated by miR-188-3p in Min6 cells (Figure 4C). On the contrary, TUG1 could positively regulate FGF5 level, showing a positive correlation (Figure 4D, 4E).

## Discussion

The incidence of T2DM is rapidly elevated in the world. T2DM patients usually accompany with obesity, lipid metabolism disorder, hypertension or other metabolic disorders. Recently, dysfunction of islet  $\beta$  cells has been considered as an essential event in the pathogenesis of T2DM<sup>15</sup>. With the prolongation of T2DM, islet  $\beta$  cell function is progressively degraded<sup>16</sup>. Therefore, protecting islet  $\beta$  cell function is conducive to alleviate the progression of T2DM.

LncRNAs are upstream key factors responsible for regulating gene expressions<sup>17,18</sup>. They



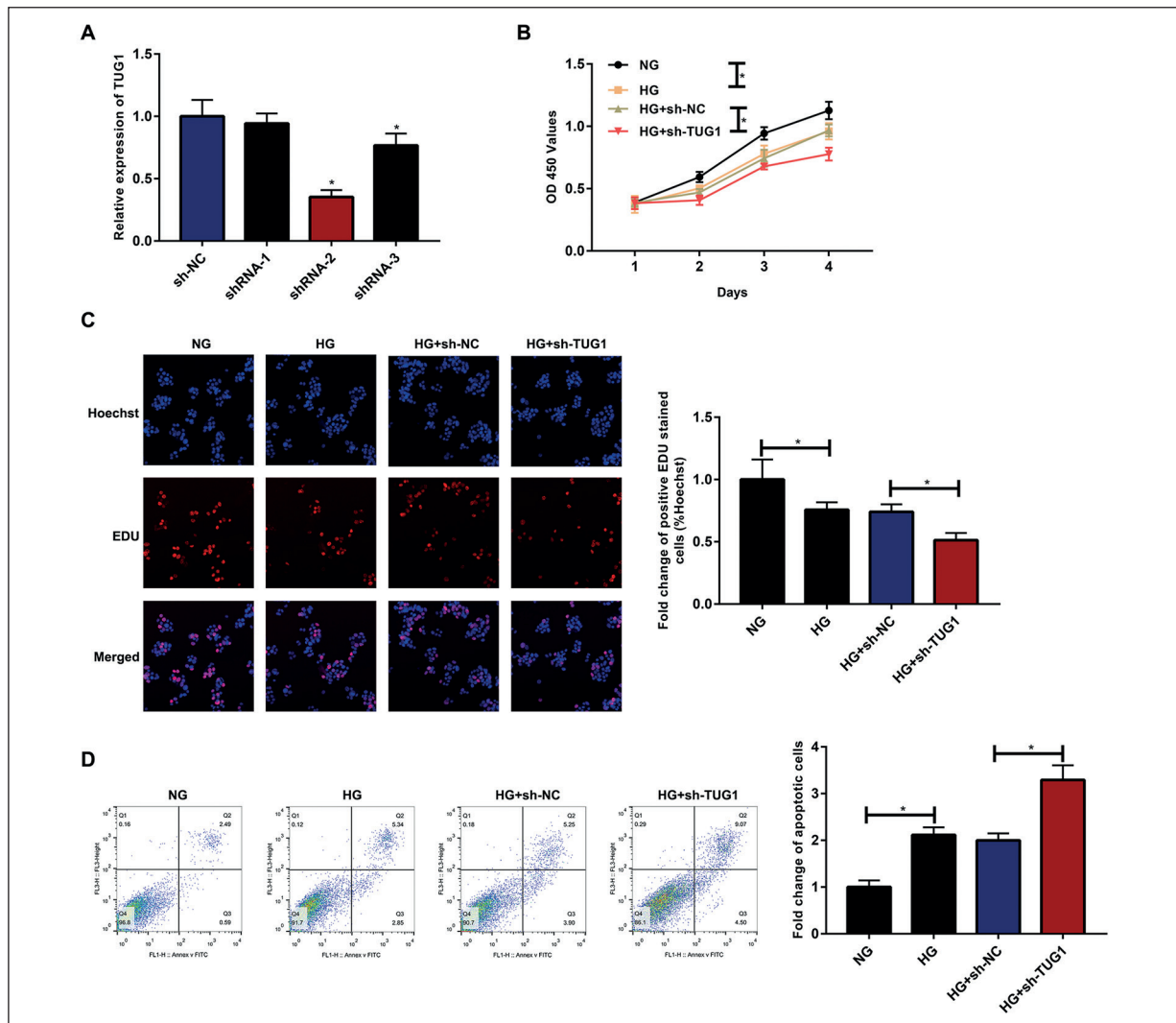


**Figure 2.** Knockdown of TUG1 inhibited proliferative ability in HG-induced Min6 cells and induced apoptosis. **A**, Transfection efficacy of three lines of TUG1 shRNA in Min6 cells. **B**, Viability in NG or HG-induced Min6 cells transfected with sh-TUG1. **C**, EdU-positive rate in NG or HG-induced Min6 cells transfected with sh-TUG1, (magnification: 200×) **D**, Apoptosis rate in NG or HG-induced Min6 cells transfected with sh-TUG1; \* $p < 0.05$ .

are extensively involved in cell behaviors<sup>19-21</sup> and highly specific based on cell types and target regulations<sup>22</sup>. As a result, lncRNAs may become potential predictable biomarkers and therapeutic targets. Abnormally expressed lncRNAs in tumor cells can priorly reflect pathological states than protein-encoding RNAs<sup>23,24</sup>. In high-fat and high-glucose models, we found that TUG1 was downregulated, indicating the potential involvement of TUG1 in the regulation of islet  $\beta$  cell functions.

LncRNA TUG1 downregulates miR-377 by the sponge effect, and thus alleviates the inhibitory effect of miR-377 on PPAR $\gamma$  activity. The TUG1/miR-377/PPAR $\gamma$  axis is involved in the onset of

diabetic nephropathy (DN) by reducing ECM accumulation in mesangial cells<sup>25</sup>. Gene sequencing identified the differentially expressed TUG1 in DN profiling<sup>26</sup>. Overexpression of TUG1 in podocytes of DN mice improves DN-associated biochemical and histological characteristics by binding PGC-1 $\alpha$ . Our results suggested that knockdown of TUG1 inhibited proliferative ability and induced apoptosis in high-glucose-treated Min6 cells.

Serving as a transcription factor, SP1 participates in lncRNA transcription. Qi et al<sup>27</sup> showed that SP1 activates the expression of lncRNA AGAP2-AS1 in gastric cancer cells. Liu et al<sup>28</sup> demonstrated that SP1 upregulates lncRNA SNHG14 in clear

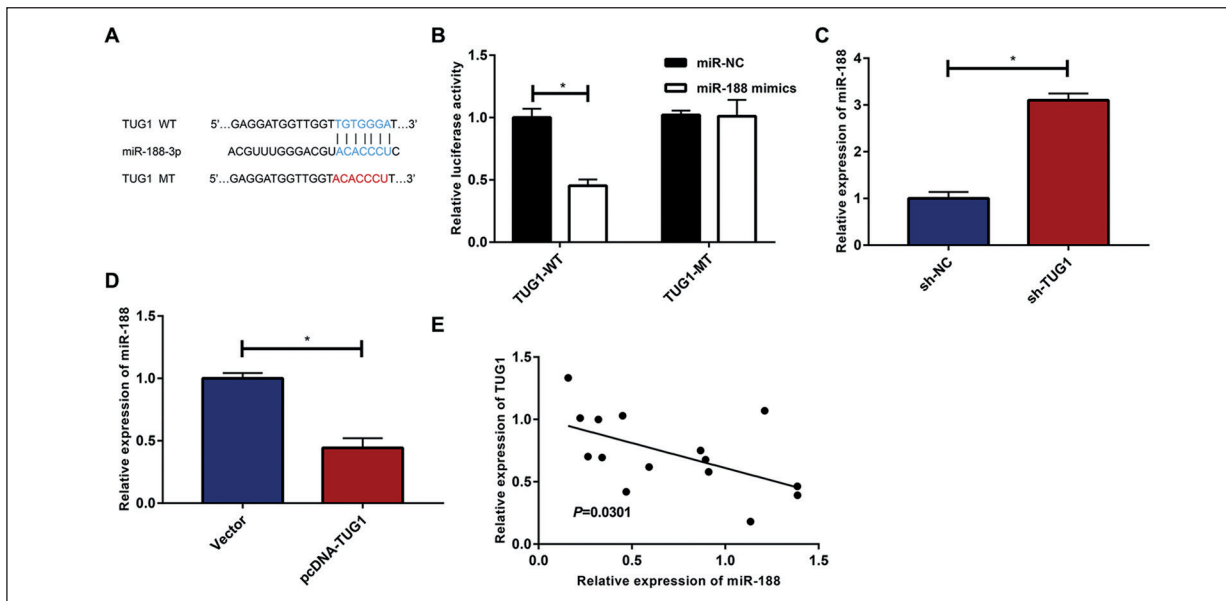


**Figure 3.** TUG1 negatively regulated miR-188-3p level. **A**, Binding sites in the seed sequence of TUG1 and miR-188-3p. **B**, Luciferase activity in wild-type and mutant-type TUG1 vectors regulated by miR-188-3p. **C**, MiR-188-3p level in Min6 cells transfected with sh-TUG1. **D**, MiR-188-3p level in Min6 cells transfected with pcDNA-TUG1. **E**, A negative correlation between TUG1 and miR-188-3p levels in mouse islet of HFD group analyzed by Spearman's rank correlation coefficient;  $*p<0.05$ .

cell renal cell carcinoma. Our findings revealed the downregulation of SP1 in high-fat and high-glucose models. Furthermore, we have proven the interaction between SP1 and TUG1.

Meng et al<sup>29</sup> reported that knockdown of miR-188-3p attenuates proliferative, migratory and invasive potentials in glioblastoma cells. As the novel negative regulator for TMED3, miR-188-3p

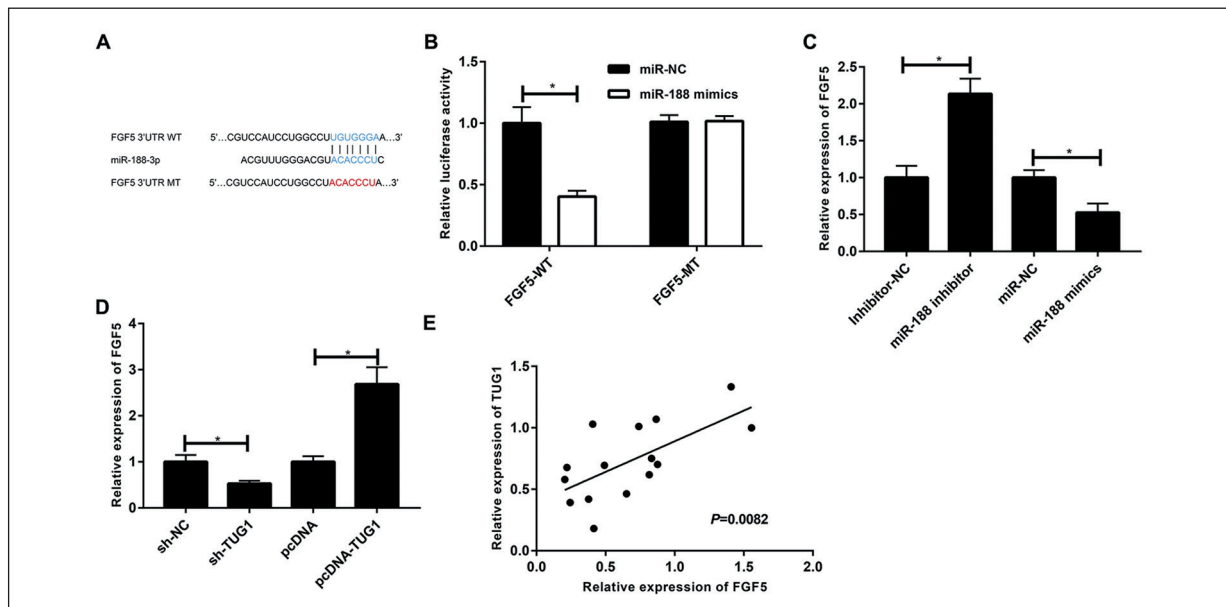


**Figure 4.** MiR-188-3p negatively regulated FGF5. **A**, Binding sites in the seed sequence of FGF5 and miR-188-3p. **B**, Luciferase activity in wild-type and mutant-type FGF5 vectors regulated by miR-188-3p. **C**, FGF5 level in Min6 cells regulated by miR-188-3p. **D**, FGF5 level in Min6 cells regulated by TUG1. **E**, A positive correlation between TUG1 and FGF5 levels in mouse islet of HFD group analyzed by Spearman's rank correlation coefficient;  $*p<0.05$ .

alleviates proliferative and metastatic capacities in breast cancer cells<sup>30</sup>. In this paper, we identified the TUG1/miR-188-3p/FGF5 axis, which was responsible for regulating proliferative and apoptotic abilities in Min6 cells. However, rescue experiments by intervening TUG1 level are not conducted, which will be further completed.

## Conclusions

The results of this study demonstrated that SP1 induces TUG1 downregulation in T2DM cell models, which further regulates proliferative and apoptotic potentials in islet cells by activating the miR-188-3p / FGF5 axis and provides a novel target for gene therapy in the future.

## Conflict of Interest

The Authors declare that they have no conflict of interests.

## References

- 1) Saisho Y. Beta-cell dysfunction: its critical role in prevention and management of type 2 diabetes. *World J Diabetes* 2015; 6: 109-124.
- 2) Zhu Y, Liu Q, Zhou Z, Ikeda Y. PDX1, Neurogenin-3, and MAFA: critical transcription regulators for beta cell development and regeneration. *Stem Cell Res Ther* 2017; 8: 240.
- 3) Petrenko V, Saini C, Giovannoni L, Gobet C, Sage D, Unser M, Heddad MM, Gu G, Bosco D, Gachon F, Philippe J, Dibner C. Pancreatic alpha-cellular and beta-cellular clocks have distinct molecular properties and impact on islet hormone secretion and gene expression. *Genes Dev* 2017; 31: 383-398.
- 4) Wang X, Sterr M, Burtscher I, Chen S, Hieronimus A, Machicao F, Staiger H, Haring HU, Lederer G, Meitinger T, Cernilogar FM, Schotta G, Irmeler M, Beckers J, Hrabe DAM, Ray M, Wright C, Bakhti M, Lickert H. Genome-wide analysis of PDX1 target genes in human pancreatic progenitors. *Mol Metab* 2018; 9: 57-68.
- 5) Cropano C, Santoro N, Groop L, Dalla MC, Cobelli C, Galderisi A, Kursawe R, Pierpont B, Goffredo M, Caprio S. The rs7903146 variant in the TCF7L2 gene increases the risk of prediabetes/Type 2 diabetes in obese adolescents by impairing beta-cell function and hepatic insulin sensitivity. *Diabetes Care* 2017; 40: 1082-1089.
- 6) Gao ZQ, Wang JF, Chen DH, Ma XS, Yang W, Zhe T, Dang XW. Long non-coding RNA GAS5 antagonizes the chemoresistance of pancreatic cancer cells through down-regulation of miR-181c-5p. *Biomed Pharmacother* 2018; 97: 809-817.
- 7) Li TF, Liu J, Fu SJ. The interaction of long non-coding RNA MIAT and miR-133 play a role in the proliferation and metastasis of pancreatic carcinoma. *Biomed Pharmacother* 2018; 104: 145-150.
- 8) Brosnan CA, Voinnet O. The long and the short of noncoding RNAs. *Curr Opin Cell Biol* 2009; 21: 416-425.
- 9) Matera AG, Terns RM, Terns MP. Non-coding RNAs: lessons from the small nuclear and small nucleolar RNAs. *Nat Rev Mol Cell Biol* 2007; 8: 209-220.
- 10) Moran I, Akerman I, van de Bunt M, Xie R, Benazra M, Nammo T, Arnes L, Nakic N, Garcia-Hurtado J, Rodriguez-Segui S, Pasquali L, Sauty-Colace C, Beucher A, Scharfmann R, van Arensbergen J, Johnson PR, Berry A, Lee C, Harkins T, Gmyr V, Pattou F, Kerr-Conte J, Piemonti L, Berney T, Hanley N, Gloyn AL, Susse L, Langman L, Brayman KL, Sander M, McCarthy MI, Ravassard P, Ferrer J. Human beta cell transcriptome analysis uncovers lncRNAs that are tissue-specific, dynamically regulated, and abnormally expressed in type 2 diabetes. *Cell Metab* 2012; 16: 435-448.
- 11) Bramswig NC, Everett LJ, Schug J, Dorrell C, Liu C, Luo Y, Streeter PR, Naji A, Grompe M, Kaestner KH. Epigenomic plasticity enables human pancreatic alpha to beta cell reprogramming. *J Clin Invest* 2013; 123: 1275-1284.
- 12) Xie C, Chen B, Wu B, Guo J, Cao Y. LncRNA TUG1 promotes cell proliferation and suppresses apoptosis in osteosarcoma by regulating miR-212-3p/FOXA1 axis. *Biomed Pharmacother* 2018; 97: 1645-1653.
- 13) Yang G, Yin H, Lin F, Gao S, Zhan K, Tong H, Tang X, Pan Q, Gou X. Long noncoding RNA TUG1 regulates prostate cancer cell proliferation, invasion and migration via the Nrf2 signaling axis. *Pathol Res Pract* 2020; 216: 152851.
- 14) Shen X, Hu X, Mao J, Wu Y, Liu H, Shen J, Yu J, Chen W. The long noncoding RNA TUG1 is required for TGF-beta/TWIST1/EMT-mediated metastasis in colorectal cancer cells. *Cell Death Dis* 2020; 11: 65.
- 15) Wang L, Gao P, Zhang M, Huang Z, Zhang D, Deng Q, Li Y, Zhao Z, Qin X, Jin D, Zhou M, Tang X, Hu Y, Wang L. Prevalence and ethnic pattern of diabetes and prediabetes in China in 2013. *JAMA* 2017; 317: 2515-2523.
- 16) Hayes AJ, Leal J, Gray AM, Holman RR, Clarke PM. UKPDS outcomes model 2: a new version of a model to simulate lifetime health outcomes of patients with type 2 diabetes mellitus using data from the 30 year United Kingdom Prospective Diabetes Study: UKPDS 82. *Diabetologia* 2013; 56: 1925-1933.
- 17) Nanditha A, Ma RC, Ramachandran A, Snehalatha C, Chan JC, Chia KS, Shaw JE, Zimmet PZ. Diabetes in Asia and the Pacific: implications for the global epidemic. *Diabetes Care* 2016; 39: 472-485.

- 18) Liang Z, Ren C. Emodin attenuates apoptosis and inflammation induced by LPS through up-regulating lncRNA TUG1 in murine chondrogenic ATDC5 cells. *Biomed Pharmacother* 2018; 103: 897-902.
- 19) Chu J, Li H, Xing Y, Jia J, Sheng J, Yang L, Sun K, Qu Y, Zhang Y, Yin H, Wan J, He F. LncRNA MNX1-AS1 promotes progression of esophageal squamous cell carcinoma by regulating miR-34a/SIRT1 axis. *Biomed Pharmacother* 2019; 116: 109029.
- 20) Jin J, Zhang S, Hu Y, Zhang Y, Guo C, Feng F. SP1 induced lncRNA CASC11 accelerates the glioma tumorigenesis through targeting FOXK1 via sponging miR-498. *Biomed Pharmacother* 2019; 116: 108968.
- 21) Hu H, Wang Y, Zhang T, Zhang C, Liu Y, Li G, Zhou D, Lu S. Association of LncRNA-GACAT3 with MRI features of breast cancer and its molecular mechanism. *J Buon* 2019; 24: 2377-2384.
- 22) Cabili MN, Trapnell C, Goff L, Koziol M, Tazon-Vega B, Regev A, Rinn JL. Integrative annotation of human large intergenic noncoding RNAs reveals global properties and specific subclasses. *Genes Dev* 2011; 25: 1915-1927.
- 23) Liu G, Xiang T, Wu QF, Wang WX. Long Noncoding RNA H19-Derived miR-675 Enhances Proliferation and Invasion via RUNX1 in Gastric Cancer Cells. *Oncol Res* 2016; 23: 99-107.
- 24) Tang T, Cheng Y, She Q, Jiang Y, Chen Y, Yang W, Li Y. Long non-coding RNA TUG1 sponges miR-197 to enhance cisplatin sensitivity in triple negative breast cancer. *Biomed Pharmacother* 2018; 107: 338-346.
- 25) Duan LJ, Ding M, Hou LJ, Cui YT, Li CJ, Yu DM. Long noncoding RNA TUG1 alleviates extracellular matrix accumulation via mediating microRNA-377 targeting of PPARgamma in diabetic nephropathy. *Biochem Biophys Res Commun* 2017; 484: 598-604.
- 26) Long J, Badal SS, Ye Z, Wang Y, Ayanga BA, Galvan DL, Green NH, Chang BH, Overbeek PA, Danesh FR. Long noncoding RNA Tug1 regulates mitochondrial bioenergetics in diabetic nephropathy. *J Clin Invest* 2016; 126: 4205-4218.
- 27) Qi F, Liu X, Wu H, Yu X, Wei C, Huang X, Ji G, Nie F, Wang K. Long noncoding AGAP2-AS1 is activated by SP1 and promotes cell proliferation and invasion in gastric cancer. *J Hematol Oncol* 2017; 10: 48.
- 28) Liu G, Ye Z, Zhao X, Ji Z. SP1-induced up-regulation of lncRNA SNHG14 as a ceRNA promotes migration and invasion of clear cell renal cell carcinoma by regulating N-WASP. *Am J Cancer Res* 2017; 7: 2515-2525.
- 29) Meng L, Jiang YP, Zhu J, Li B. MiR-188-3p/GPR26 modulation functions as a potential regulator in manipulating glioma cell properties. *Neurol Res* 2020; 42: 222-227.
- 30) Pei J, Zhang J, Yang X, Wu Z, Sun C, Wang Z, Wang B. TMED3 promotes cell proliferation and motility in breast cancer and is negatively modulated by miR-188-3p. *Cancer Cell Int* 2019; 19: 75.